

Supplementary Information

Highly Stretchable and Sensitive Piezoresistive Carbon Nanotube /Elastomeric Triisocyanate-Crosslinked Polytetrahydrofuran Nanocomposites

Yunming Wang^{§a}, Hongyi Mi^{§b}, Qifeng Zheng^a, Huilong Zhang,^b Zhenqiang Ma^{*b}, and Shaoqin Gong^{*a}

^aDepartment of Biomedical Engineering, Wisconsin Institute for Discovery, and Materials Science Program, University of Wisconsin–Madison, Madison, WI 53706, USA

^bDepartment of Electrical and Computer Engineering, University of Wisconsin–Madison, Madison, WI 53706, USA

[§]These authors contributed equally to this work.

*Corresponding authors: mazq@engr.wisc.edu, Tel: +1-608-261-1095;
sgong@engr.wisc.edu, Tel: +1-608-316-4311.

Materials

Multi-walled carbon nanotubes (CNTs) (inner diameter: 4 nm, length: >1 μm , number of walls: 3–15, bulk density: 140–230 kg/m^3 , purity: > 99 %) were kindly provided by Bayer Materials Science AG, 51368 Leverkusen, Germany. Triphenylmethanetriisocyanate (TTI, Boc Sciences, NY, USA) and dibutyltin dilaurate (DBT, Alfa Aesar, MA, USA) were used as received. The materials p-anisidine, sodium dodecyl sulfonate, and toluene were purchased from Fisher Scientific (Bellefonte, PA). Polytetrahydrofuran (PTHF 2.9 kDa) was purchased from Sigma-Aldrich (St. Louis, MO). PTHF 2.9 kDa was dried at 100 °C under a high vacuum (0.010 MPa) for 2 h before use. Toluene was dried for 48 h using a 5 Å

molecular sieve and then distilled prior to use. All other reagents were of analytical grade and were used as received.

Structural Analyses

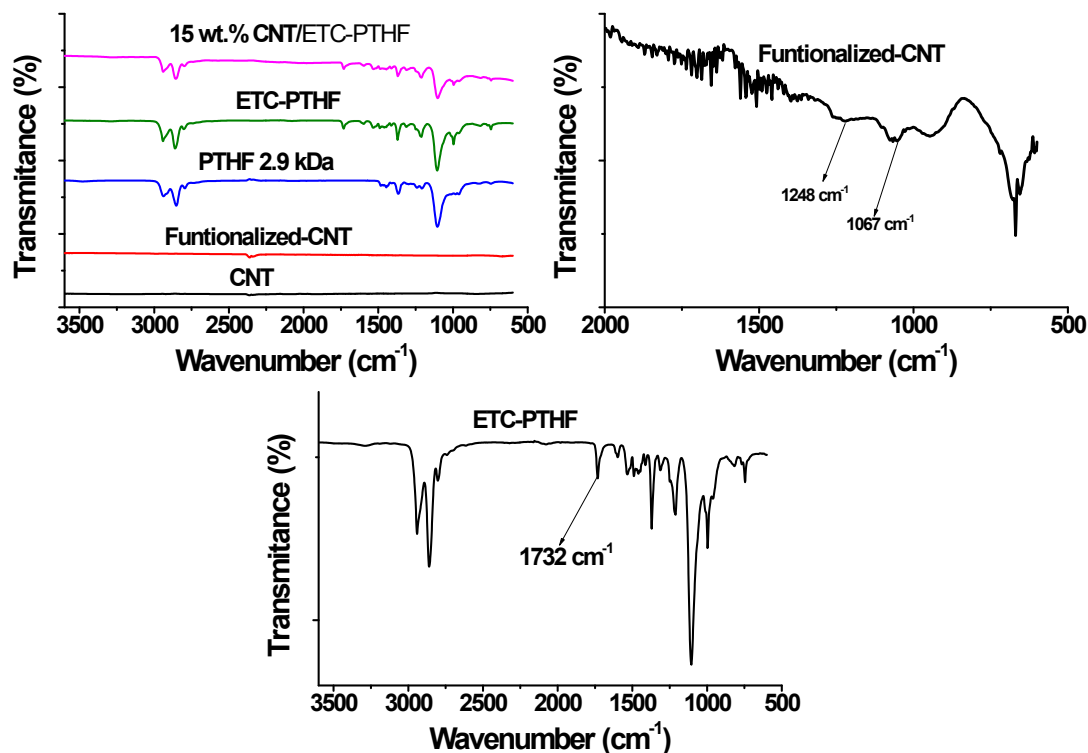


Fig. S1 The FTIR spectra of the CNTs, surface-functionalized CNTs, PTHF 2.9 kDa, ETC-PTHF, and CNT/ETC-PTHF nanocomposites.

CNT: No peaks appeared between 1500 and 1800 cm^{-1} .

Surface-functionalized CNT: FT-IR (Fig. S1): 1598 and 1506 (ν C=C aromatic) cm^{-1} , 1248 (ν_{as} CH₃O-Ar) cm^{-1} , and 1067 (ν_{s} CH₃O-Ar) cm^{-1} .

ETC-PTHF: 2941 and 2860 (ν CH₂) cm^{-1} , 1732 (ν C=O) cm^{-1} , 1598 and 1490 (ν C=C aromatic) cm^{-1} , 1460 and 1447 (δ_{as} CH₂) cm^{-1} , 1371 (ν_{as} C-N aromatic) cm^{-1} , 1313 (δ_{s} CH₂) cm^{-1} , 1212 (ν_{as} C-O-C) cm^{-1} , and 1106 (ν_{s} C-O-C) cm^{-1} .

15 wt.% CNT/ETC-PTHF nanocomposite: 2940 and 2855 (ν CH₂) cm^{-1} , 1731 (ν C=O) cm^{-1} , 1597 and 1486 (ν C=C aromatic) cm^{-1} , 1532 (ν C=C aromatic, functionalized CNT) cm^{-1} ,

1458 and 1446 (δ_{as} CH₂) cm⁻¹, 1370 (ν_{as} C-N aromatic) cm⁻¹, 1311 (δ_s CH₂) cm⁻¹, 1211 (ν_{as} C-O-C) cm⁻¹, and 1103 (ν_s C-O-C) cm⁻¹.

Electrical Conductivity Measurements

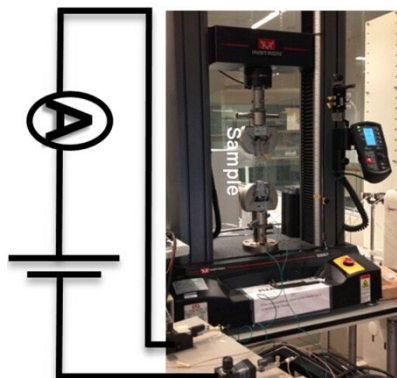


Fig. S2 A schematic representation of the experimental setup used to measure the electrical conductivity regulated under different strains.

Poisson Ratio

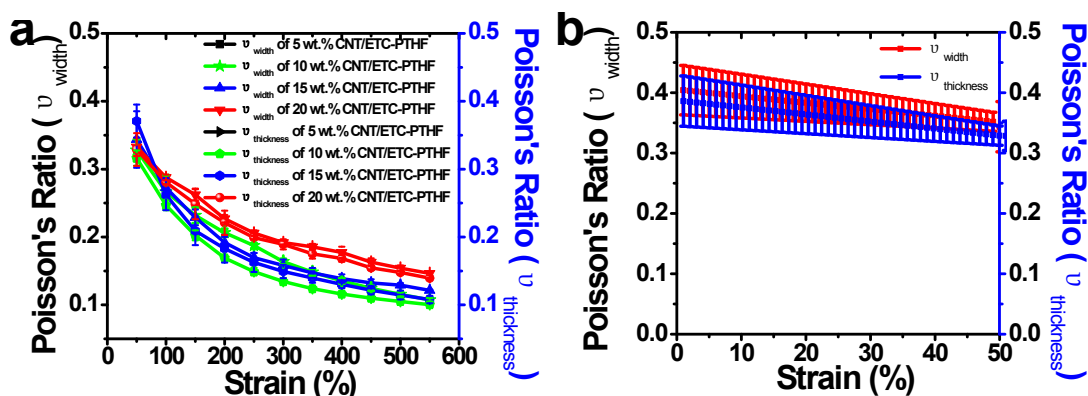


Fig. S3 (a) The Poisson ratios of the CNT/ETC-PTHF nanocomposites with various CNT loading contents (5 to 20%) which were measured from both width change (left, ν_{width}) and thickness change (right, $\nu_{thickness}$) as a function of tensile strain (large strain region ranging from 50% to 550%); **(b)** The Poisson ratios of the 15 wt.% CNT/ETC-PTHF as a function of the tensile strains (low strain region ranging from 1% to 50%).

Derivation of the Equation Used to Calculate the Conductivity

σ

$$\begin{aligned}
 &= \frac{1}{\rho} = \frac{1}{RWT} = \frac{L_0 + \Delta L}{R(w_0 + \Delta w)(T_0 + \Delta T)} = G \frac{L_0 \left(1 + \frac{\Delta L}{L_0}\right)}{W_0 T_0 \left(1 + \frac{\Delta w}{w_0}\right) \left(1 + \frac{\Delta T}{T_0}\right)} = G \frac{L_0(1 + \varepsilon_L)}{W_0 T_0 (1 + \varepsilon_w)(1 + \varepsilon_T)} = G \\
 &= G \frac{L_0(1 + \varepsilon_L)}{W_0 T_0 \varepsilon_L^2 \left(\frac{1}{\varepsilon_L} - \nu_{thickness}\right) \left(\frac{1}{\varepsilon_L} - \nu_{width}\right)} \\
 &= G \frac{L_0(1 + \varepsilon_L)}{W_0 T_0 (1 - \varepsilon_L \nu_{thickness}) (1 - \varepsilon_L \nu_{width})} \quad (S1)
 \end{aligned}$$

where σ is the conductivity of the stretchable CNT/ETC-PTHF nanocomposites, G is the conductance of the stretchable CNT/ETC-PTHF nanocomposite, and ε_L is the longitude direction strain. The parameters L_0 , T_0 , and W_0 are the initial length, thickness, and width of the sample, respectively. The parameter $\nu_{thickness}$ is the Poisson's ratio of thickness and ν_{width} is the Poisson's ratio of width.

Thermal Stability

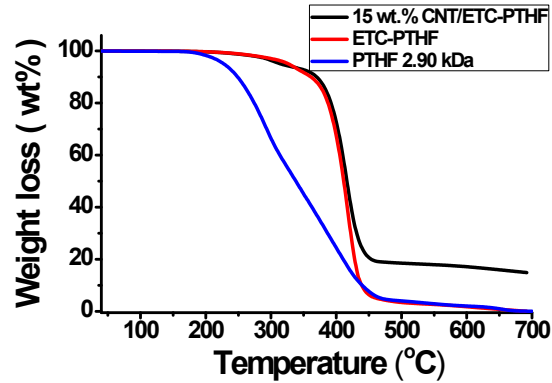


Fig. S4 The thermogravimetric analysis (TGA) curves of PTHF (2.9 kDa), ETC-PTHF, and 15 wt.% CNT/ETC-PTHF nanocomposites.

The TGA curves of PTHF (2.9 kDa), ETC-PTHF and 15 wt.% CNT/ETC-PTHF nanocomposites are shown in Fig. S4. The most significant weight loss occurred between 394 and 421 °C, which was attributed to the degradation of the PTHF chains. Compared with the char yield of ETC-PTHF, the 15 wt.% CNT/ETC-PTHF nanocomposite produced

approximately 15 wt.% more carbonaceous residues after thermal degradation, which was equivalent to the amount of CNTs incorporated in the CNT/ETC-PTHF nanocomposite.

Mechanical Properties

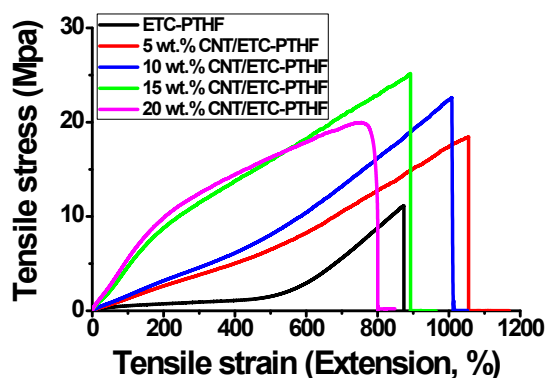


Fig. S5 The tensile stress–strain curves of the CNT/ETC-PTHF nanocomposites (according to ASTM: D882).

Table S1 Mechanical properties of the CNT/ETC-PTHF nanocomposites.

Samples	Tensile strength-at-break (MPa)	Tensile strain-at-break (mm/mm)	Young's modulus (E-modulus) (MPa)
ETC-PTHF	11.14 ± 0.87	8.74 ± 1.92	0.78 ± 0.04
5 wt.% CNT/ETC-PTHF	18.42 ± 2.32	10.56 ± 2.14	1.25 ± 0.06
10 wt.% CNT/ETC-PTHF	25.35 ± 3.01	10.09 ± 1.32	1.72 ± 0.03
15 wt.% CNT/ETC-PTHF	25.16 ± 1.62	8.92 ± 1.39	4.26 ± 0.11
20 wt.% CNT/ETC-PTHF	19.97 ± 3.08	7.54 ± 1.77	5.04 ± 0.04

Differential Scanning Calorimetry (DSC) Analyses

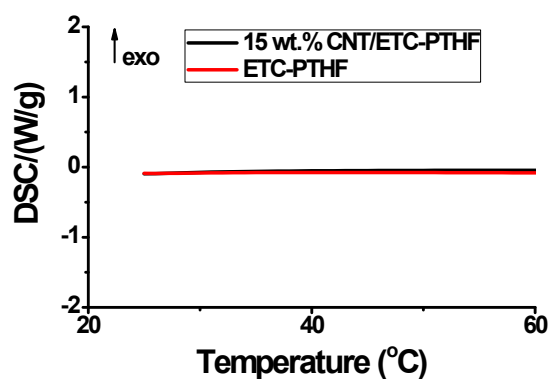


Fig. S6 DSC for 15 wt.% CNT/ETC-PTHF nanocomposite and ETC-PTHF measured from room temperature (first round DSC).

Scherrer Equation

The effective crystallite size L in the PTHF-based nanocomposites was estimated from Scherrer's equation,¹

$$L = \frac{\alpha\lambda}{\beta\cos\theta_m} \quad (\text{S2})$$

where α is the coefficient accounting for the form of correlation zone ($\alpha = 2 \times (\ln 2/\pi)^{1/2} \approx 0.93$),² β is the full width at half maximum (FWHM) of the diffraction peak expressed in radians, and θ_m is half of the diffraction angle (2θ) corresponding to the position of the diffraction peak. The characteristic peaks at 19.9° and 24.4° in XRD spectra in Fig. 2c were adopted to calculate L .

Dielectric Properties

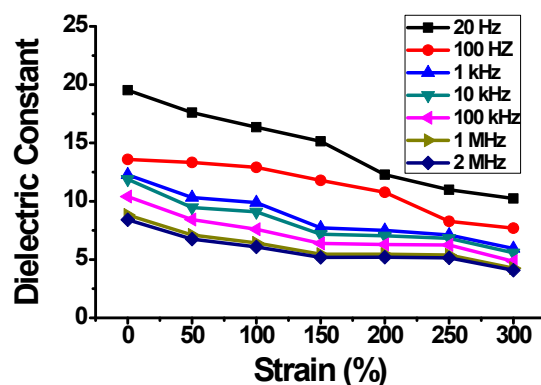


Fig. S7. The change in dielectric constant (ϵ) of 15 wt.% CNT/ETC-PTHF nanocomposite as a function of tensile strain measured at different frequencies.

Supplementary Information References

1. N. I. Lebovka, E. A. Lysenkov, A. I. Goncharuk, Y. P. Gomza, V. V. Klepko and Y. P. Boiko, *J. Compos. Mater.* **2011**, *45*, 2555.
2. A. L. Patterson, *Phys. Rev.* **1939**, *56*, 978.

